

## THE COMPARISON BETWEEN SUMMER MONSOON COMPONENTS OVER EAST ASIA AND SOUTH ASIA

Weihong QIAN and Yafen ZHU

*Department of Atmospheric Sciences, Peking University, Beijing 100871, P. R. China, qianwh@pku.edu.cn*

### Abstract

This is an observational study in which regional climatological features of the different summer monsoon components over East Asia and South Asia are compared. The data sets used are the Climate Prediction Center (CPC) Merged Analysis of Precipitation (CMAP), National Meteorological Center (NMC) global wind analysis, outgoing longwave radiation (OLR), and upper-tropospheric water vapor band brightness temperature (BT) observed from National Oceanic and Atmospheric Administration (NOAA) polar orbiting satellites. The criterion of summer monsoon onset for each variable is determined and used to compare the seasonal transition in different regions. The summer monsoon over the central South China Sea (SCS) abruptly sets up in mid May or the pentad 28 (16-20, May) of the year; it results from the combination of rain zones coming from its west, north, east and south near the equator. During this time, southwesterly monsoon flow and monsoon rainbelt establish from the equatorial Arabian Sea, the Bay of Bengal (BOB), the SCS to the northwest Pacific, which marks seasonal transition and illustrates the interconnection between the South Asian and East Asian monsoon components. After onset of the SCS summer monsoon, a convective rainbelt extends northward from the central SCS to the Yangtze River, and consequently the *Meiyu* (plus rain or monsoon rainfall) is established over central eastern China. The rainfall in India is characterized by a "Y" pattern emanating from the equator while in East Asia the rainfall is characterized by an inverted "Y" pattern in the transition process. In South and Southeast Asia, four centers of strong rainfall stand near the 73E, the 90E, the 105E, and the 117E during the summer monsoon season. In the subtropical western Pacific, the monsoon rainfall extends eastward to the east Philippines between 120E and 140E in mid June, and between 140E and 160E in mid July. Other aspects of the monsoon rainfall are also examined and compared using indices based on the BT, OLR and 850hPa-wind field.

**Key words:** South Asia / East Asia / summer monsoon / precipitation / brightness temperature / wind

### Introduction

The Asian monsoon system, prevailing from the Indian subcontinent, the Indochina Peninsula (ICP), Mainland China, the South China Sea (SCS) and the northwestern Pacific during the late boreal spring to summer, has gradually received more attentions in recent years. It has been recognized that the regional monsoon is an important component of the broad scale Asian monsoon (Webster and Yang 1992). Especially, an abrupt seasonal transition occurs in Asia associated with the onset of the SCS summer monsoon (e.g., Lau and Yang 1997; Qian and Lee 2000; Qian and Yang 2000).

According to Tao and Chen (1987), the Asian summer monsoon includes at least two subsystems: the Indian monsoon (or South Asian monsoon) and the East Asian monsoon. These subsystems are composed of different circulation components. They

affect each other strongly at some times but tend to vary independently at other times. The aspects of the strong association and weak coupling between the two regional monsoons have been respectively referred to as the "connection" and "independence" of the subsystems (Qian and Yang 2000). In spite of the findings by limited previous studies (e.g., Yang and Gutowski 1992; Lau et al. 2000), many features about the connection and independence of these regional monsoons have not been well understood.

The SCS monsoon is an important part of the East Asian monsoon and is also linked to South Asian monsoon. Since the 1990s, particularly after the international SCS Monsoon Experiment (SCSMEX), various data sets have been used to study activities of the SCS summer monsoon. A lot of studies have provided a generally accepted description of the monsoon onset process. Climatologically, date of the

SCS monsoon onset appears in mid May of the year (Lau and Yang 1997; Wu and Zhang 1998; Xie et al. 1998). However, previous studies did not show the regional independence and explain in detail the connection between the South Asian monsoon and the SCS summer monsoon as well as the monsoon in east China.

On the other hand, numerous studies (Lau and Li 1984; Krishnamurti 1985; Lau et al. 1988; Ding et al. 1996; Qian et al. 1998; Jin 1999; Kang et al. 1999) have been conducted to examine the Asian monsoon in different regions. Data sets used in previous studies are mainly the National Centers for Environmental Prediction (NCEP) reanalysis, National Meteorological Center (NMC) global analysis, and satellite-derived data from different bands such as Outgoing Longwave Radiation (OLR), High-resolution Infrared Radiation Sounders (HIRS) water vapor band brightness temperatures (BT), and Temperature of blackbody (Tbb) at cloud-top. However, a great number of questions about the regional monsoon features and the relationship between the monsoon and related rainfall patterns still remain unrevealed combining different datasets.

In this study, several data sets are used to delineate the onset process of the monsoon and address the connection and independence between South Asian and East Asian monsoon components. We will also demonstrate the importance of satellite data for obtaining a consolidated view of the onset and evolution of the monsoon. After this introduction, data source is described in section 2. Rainbelt and flow during the seasonal transition period over the Asian region are illustrated in section 3. Local rainfall and convective features from the SCS region and the Indian region are shown in section 4. Summer monsoon features revealed from different variables crossing various regions over South Asia and East Asia are compared in section 5. A conclusion is marked in sections 6.

### 1. Data Description

One data set used in this study is the pentad mean global precipitation, i.e., Climate Prediction Center (CPC) Merged Analysis of Precipitation (CMAP). The data set has been constructed based on rain gauge observations, satellite estimates and numerical model outputs (Xie and Arkin 1997). The CMAP data used in this paper is the pentad precipitation with 2.5 degrees for 1980-1995.

Low-tropospheric wind data can indicate the changes of monsoon circulation, especially over mid- to low- latitude regions. The wind information for the 850hPa level from the US NMC global analysis wind dataset is analyzed in this study. The data, with a

spatial resolution of 2.5 degrees, cover the period from 1980 to 1995. Five-day mean values for six months (March-August) of each year focusing on the domain of 20S-40N, 40E-180 are examined.

OLR, like Tbb, reflects convective activities. The relatively lower values of OLR represent deep convection. The OLR data from the US National Oceanic and Atmospheric Administration (NOAA) polar-orbiting operational satellites are also used to study monsoon convection (Xie et al. 1998). Five-day mean values calculated from the data, which is at a spatial resolution of 2.5 degrees, are analyzed in this study. The OLR data will be compared with the CMAP data in mid and low latitudes.

In recent years, remote-sensing data from High-resolution Infrared Radiation Sounders (HIRS) or water vapor band brightness temperatures (BT) observed from the US-NOAA operational polar-orbiting satellites have also been used to study the monsoon (Qian and Lee 2000; Qian et al. 2002). There are 20 channels on the HIRS. Three channels are sensitive to variations of the tropospheric water vapor. HIRS channel 12 (or HIRS12) is designed to measure the infrared radiation of water vapor in the upper troposphere (Wu et al. 1993; Bates et al. 1996). Previous studies using the HIRS12 data indicated that the ascending or descending motions might affect the total amount of water vapor in the upper troposphere. If ascending motions occur in a moisture atmosphere, the water vapor content will increase in the upper troposphere. As a result, the BT measured by satellites or the value of the HIRS12 will decrease. In the descending regions the air becomes dry and the value of the BT will increase. Thus, the values of the water vapor band BT may be considered as an indicator of vertical motion. In this study, five-day averaged (totally 73 pentads per year) BT data from 1980 to 1995, with a focus on the region between 40S and 40N are used. The data has a horizontal resolution of 2.5 degrees.

All of these datasets have been used in the monsoon study from the eastern Asian monsoon to the global monsoon (Qian and Lee 2000; Qian and Yang 2000; Qian et al. 2002). In our previous studies, three criteria are used to identify whether the summer monsoon is onset. For CMAP, the criterion of deep convective precipitation or the summer monsoon onset is about 5-6mm/day. For BT, its criterion of deep convection could be determined as around 244K. The convective criterion of OLR is about 230W/m<sup>2</sup>. These criteria are also used in this paper to compare the regional features in East Asia and South Asia.

### 2. Rainbelt and Flow

As Webster (1987) described, the dominant

characteristic of the great monsoon system, the annual cycle itself, has led the inhabitants of the monsoon regions to divide their lives, customs, and economies into two distinct phases: the "wet" and the "dry". The wet, of course, refers to the rainy season, during which warm, moist, and very disturbed winds blow inland from the oceans. The dry refers to the other half of the year, when the wind reverses bringing cool and dry air

from the hearts of the winter continents. To define the geographic extent of the monsoon, a definition of what constitutes a monsoon climate must be decided first. The most common definition uses the characteristics of the annual variation of both wind and rainfall. Here, the distribution of pentad mean precipitation over the Asian continent and Indian/Pacific ocean regions is first displayed in **Figure 1**.

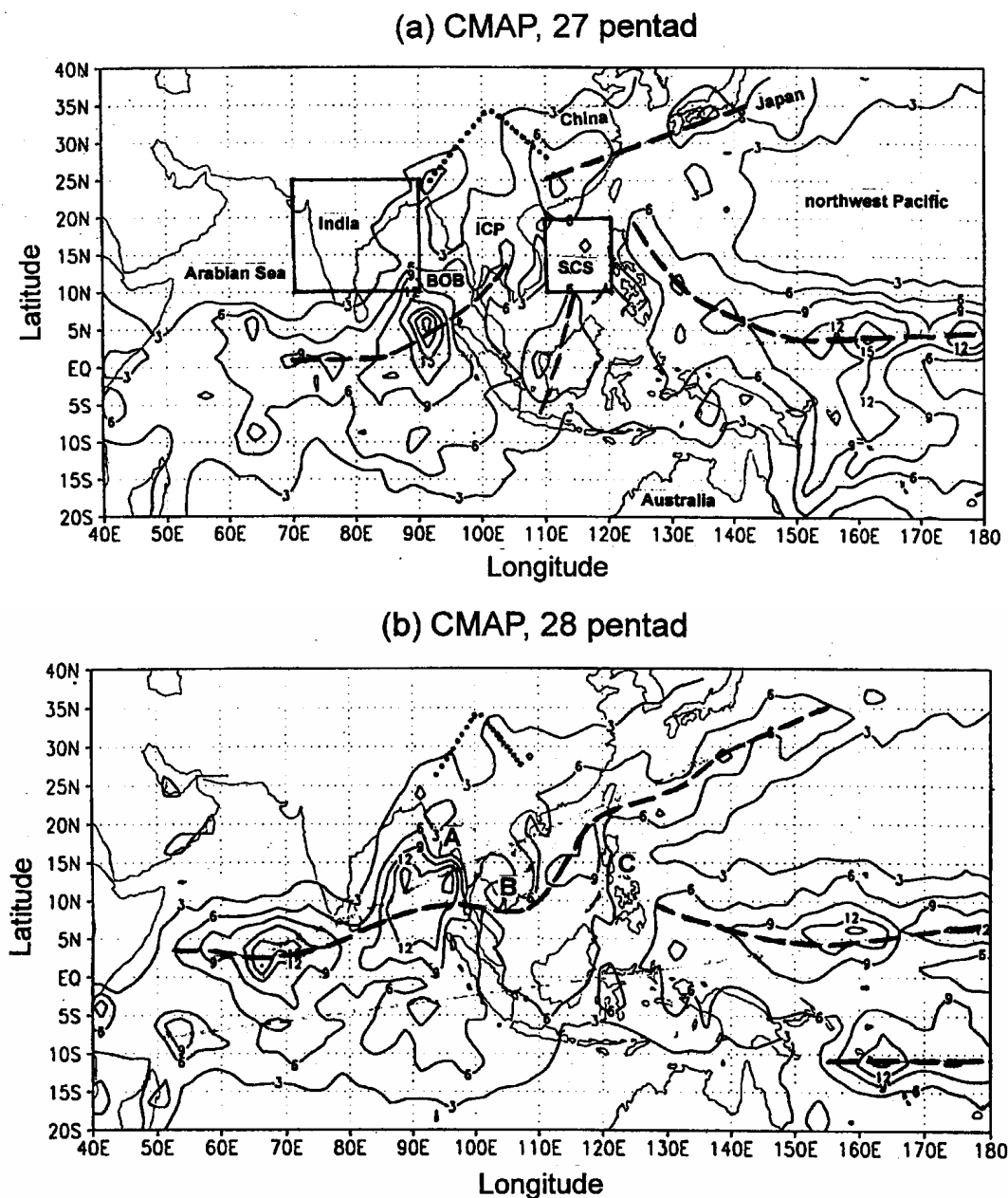


**Fig. 1** The distribution of pentad mean precipitation (CMAP; mm/day) for (a) the pentad 27 and (b) the pentad 28 of the calendar year in Asian-Australian regions. Dashed line indicates the rain zones; Dotted lines show that the precipitation is gradually decreased from south to the convergent center at central western China (35N, 100E); Two boxes shown in (a) indicate the central SCS (10N-20N, 110E-120E) and India (10N-25N, 70E-90E), respectively; "A", "B" and "C" in (b) indicate the positions of Myanmar, Cambodia and Philippines.

In the pentad 27, the relatively dry climate is situated in the central SCS region (see the SCS box). Obviously, four rainfall zones with 6mm/day have reached and surrounded the SCS box. In the west of the central SCS region, the rainfall zone is dominated from the equatorial Indian Ocean to the ICP. In its south, the rainfall zone covers the Kalimantan Island. In its east, the rainfall zone is striated from the equatorial Pacific. In its north, the rainfall zone is lined from South China to Japan.

After the onset of SCS summer monsoon, the rainfall zones are evidently modified (Fig. 1b). The original two rainfall zones in the west and the north of

the SCS box are connected to each other at the moment. The connected rainfall zone from South Asia to East Asia is likely separated from the rainfall zone in the equatorial Pacific. In the pentad 28, the SCS box occupies the precipitation with the value more than 9mm/day in its central part but the India box is still located within a dry condition.

The difference in the nature of the precipitation can also be identified from the distribution of streamlines at the 850hPa (Fig. 2). The streamline patterns at the 850hPa level in the pentad 27 are shown in Fig. 2a. Five shaded lines outline a cross-equatorial monsoon gyre in the tropical Indian Ocean, cross-equatorial flows

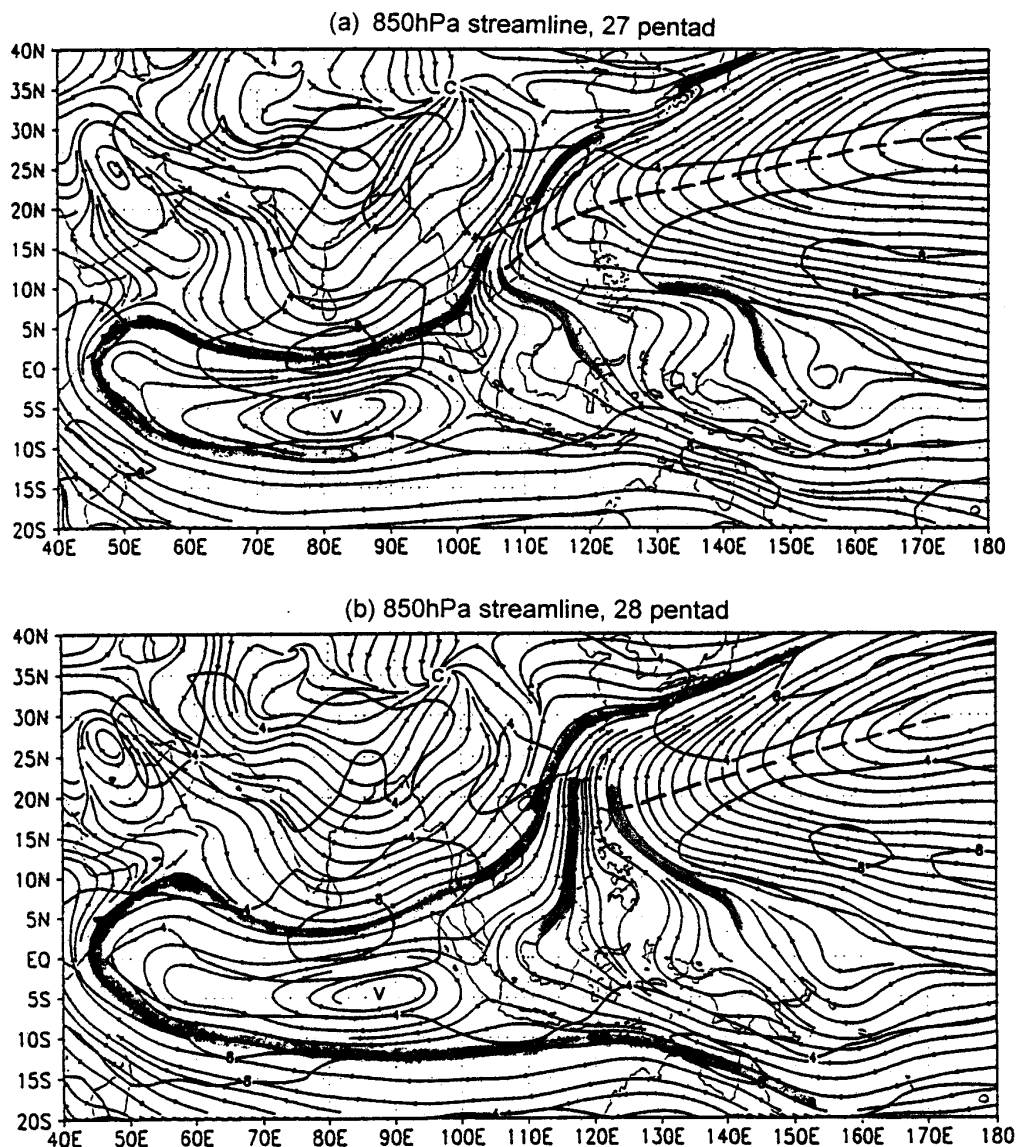


Fig. 2 Same as in Fig.1 but the 850hPa streamline and velocity (m/s) for (a) the pentad 27 and (b) the pentad 28. Dashed line indicates the ridgeline of subtropical high. Shaded lines are streamlines outlining the cross equatorial gyre or the cross-equatorial flows and frontal lows. C and V are the convergent centers and the centers of cross-equatorial gyre, respectively.

in the tropical western Pacific, and frontal flows in South China and Japan, respectively. These places with the shaded lines show the relatively strong winds and converge more vapors. These shaded lines in **Fig. 2a** are well illustrated the rainfall zones surrounding the SCS box in the 27 pentad. Accompanying these cross-equatorial flows, the rainfall zones in the tropical SCS region reflect the expansions of wet atmosphere coming from the tropical vapor centers (Qian et al. 2002). Two rainfall centers in South China and Japan are resulted from the frontal processes in the northwest of the subtropical high. Therefore, the nature of rainfall zone in South China is different from that in the tropics.

After the SCS monsoon onset (**Fig. 2b**), the subtropical high ridge has retreated eastward from the central SCS. The domain and the width of the cross-equatorial monsoon gyre are also enlarged if the shaded lines in **Fig. 2a** and **Fig. 2b** are compared. The shaded streamline from the equatorial Indian Ocean through SCS and South China to Japan can be referred to as the southwesterly monsoon flow because the flow comes from the equator. Accompanying the monsoon flow, the precipitation from the equatorial Arabian Sea, the BOB and SCS to the south of Japan in the northwest Pacific can be referred to as the monsoon rainbelt that is shown in **Fig. 1b**. The rainbelt would advance northward attributable to the strengthening of southwesterly monsoon flow. It can be noted from the description above that the connection ligament between the South Asian monsoon and the East Asian monsoon is the southwesterly monsoon flow.

Besides the southwesterly monsoon flow, another two cross-equatorial flows can also be observed along the 115E and in the equatorial western Pacific (shaded lines in **Fig. 2b**). Obviously, three cross-equatorial flows become combination in the SCS and East Asia. The three flows play an important and independent role in the regional features of the monsoon over South Asia, the SCS region, and East Asia, respectively. Due to the regional heating contrast between the continent and the ocean, three flows should have an interannual variability, resulting the interannual variability of the regional rainfall.

In the Asian continent, the place of flow convergence is the center of heating (35N, 100E) over the Asian continent in this season (Wang and Qian 1999). The southwesterly monsoon flow will gradually strengthen and advance northward after the onset of SCS summer monsoon. However, the speeds of northward advance are different over South Asia and East Asia due to the strength of local heating and topographical forcing. As indicated by the dotted line over western China in **Fig.1** and the streamlines in

**Fig. 2**, the precipitation is gradually decreased from south to the convergent center due to the increasing height of topography and the decreasing water vapor content along the streamlines. It was found that the monsoon rainfall is complex caused by the various regional circulation and their variations.

### 3. Local Rainfall in the SCS and India

Although the southwesterly monsoon flow and the monsoon rainbelt from the equatorial Indian Ocean to East Asia have formed, the Indian box is still controlled by the northwesterly flows in the pentad 28. The SCS box is located in the Southeast Asian region while the Indian box is situated in the South Asian region. We first compare the regional features of rainfall from these two boxes with season. **Figure 3** shows the climatological mean time series of four variables in the two boxes. **Fig. 3a** depicts four time series of area-averaged CMAP, HIRS (or BT), OLR and the 850hPa zonal wind (UWIND) in the SCS box while **Fig. 3b** shows that of the Indian box. All time series in **Fig. 3a** clearly indicate an abrupt change around pentad 28 or mid-May from all variables. This means that summer monsoon over the central SCS abruptly bursts in the pentad 28. This onset date has been described in previous study (Qian and Lee 2000). According to this abrupt change, the criterion of each variable to indicate the deep convection over the central SCS can be determined. For CMAP, it abruptly increases from about 4mm/day in the pentad 27 to 8mm/day in the pentad 28 so that the criterion of deep convective precipitation can be about 4-6mm/day. For HIRS, its criterion of deep convection can be determined in around 244K. The convective criterion of OLR is about  $230\text{Wm}^2$ . The onset date of SCS monsoon can be defined as the time when the area-averaged 850hPa zonal wind changes from easterly to westerly. To identify whether these criteria can be used in other regions, **Fig. 3b** and **Fig. 3a** are compared. In **Fig. 3b**, all time series have an abrupt change around pentad 31 or early June. The criteria over the Indian box are similar to those of the central SCS region except the zonal wind. According to the onset date of Indian summer monsoon, the criterion of westerly wind at the Indian region can be determined as  $5-6\text{ms}^{-1}$ . Consequently, one can use the criteria based on CMAP, HIRS and OLR to define monsoon onset, since these indices are better related.

The dry period and wet period in the annual cycle can be found from different lengths in the SCS region and the Indian region. In the SCS region the wet or the summer monsoon period starts from mid May and ends in the late of October. In the Indian region the summer monsoon can be identified from early June to

## Weihong QIAN: The Comparison between Summer Monsoon Components

late September. It is noted that the SCS summer monsoon onset is earlier and its withdrawal is later related to that of the Indian monsoon. In the Indian

region, two major peaks of rainfall appear in the monsoon period while more peaks are found in the central SCS region.

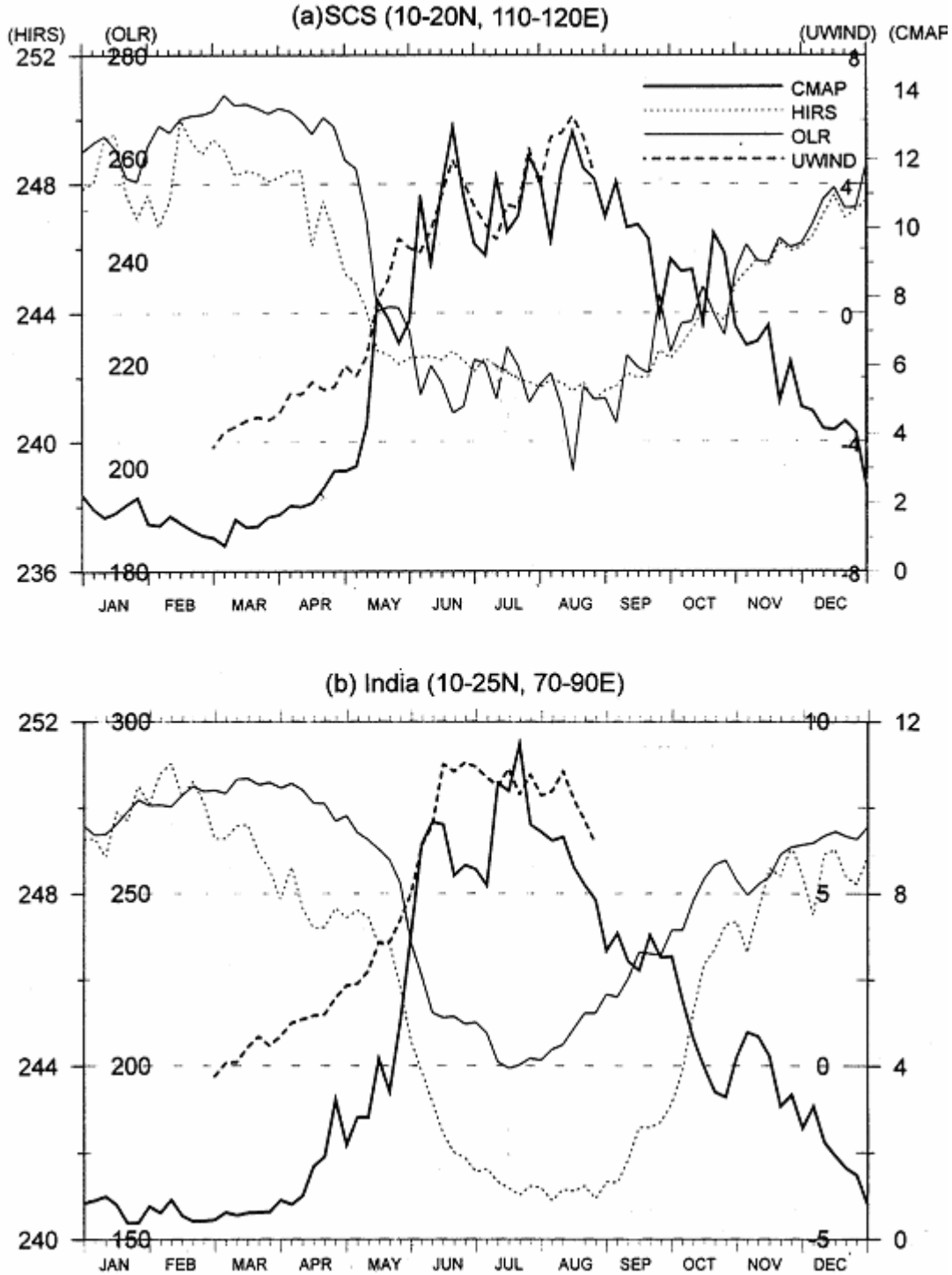


**Fig. 3** The mean time series of CMAP (mm/day), HIRS (K), OLR (W/m<sup>2</sup>), and 850hPa zonal wind (UWIND, m/s) averaged over (a) the central SCS (10N-20N, 110E-120E), and (b) India (10N-25N, 70E-90E)

## 4. Summer Monsoon Revealed from Different Variables

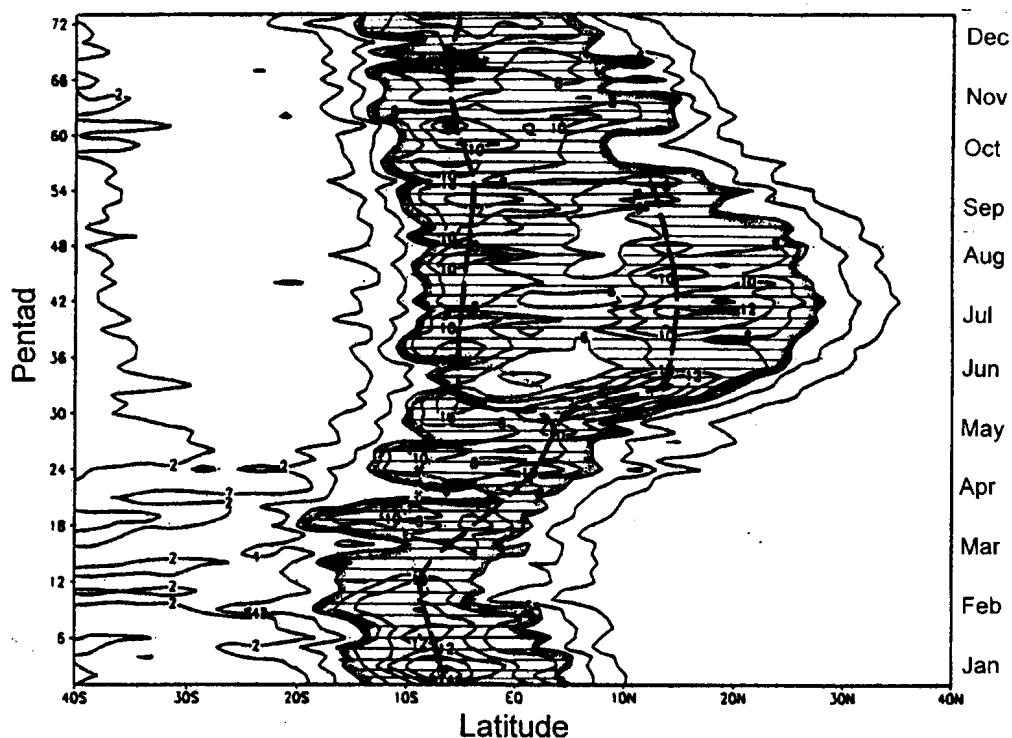
### 4.1 Precipitation

Rainfall or dry/wet alternation at a local area is an important indicator for the summer monsoon onset. **Figure 4** depicts the distributions of rainfall along different latitude and longitude sections with season. The precipitation averaged between 70E and 90E with the total 73 pentads a year is shown in **Fig. 4a**. Along the longitude, the precipitation mainly appears to the south of the equator. Between 10S and the equator, the precipitation is always maintained, while between the equator and 28N, there is a transition of rainfall/non-rainfall with season. In the southern tip of the Indian subcontinent (10N), the rainfall maximum starts from the pentad 31 then rapidly extends northward to about 15N at the pentad 33 (mid-June), so that the mean onset of the Indian summer monsoon is also very rapid within two pentads. The rainfall that is characterized by a "Y" pattern emanating from the equator can be identified in the transition season. The "Y" pattern indicates that a maximum of precipitation near the equator occurs in April and May then splits into two maxima after the monsoon onset. For the Indian summer monsoon, one of two maxima near 15N should be noted. This rainfall maximum rapidly extends northward in early June then remains at 15N for the whole summer.

The average rainfall between 110E and 120E along the longitude of the SCS is more complex. From **Fig. 4b**, the maximum of rainfall in boreal winter period is located in the south of the equator near 6S. In boreal spring two maxima of rainfall appear over the equator and subtropical South China (27N) while a dry region occurs in the central SCS between 10N and 20N. From mid-May, two maxima of precipitation rapidly concentrate toward the central SCS and are maintained through to autumn. Another feature can be found in East China from mid-June (33 pentad) to mid-July (39 pentad): a maximum of precipitation rapidly extends northward from the central SCS, through South China to the Yangtze River. The maximum of precipitation that remains at 30N about one month from mid-June to mid-July is an indicator of Meiyu (summer monsoon rainfall in the lower Yangtze River). It can be easily identified from before to after the SCS monsoon onset that the precipitation exhibits an inverted "Y" pattern if comparing it with the "Y" pattern in **Fig.4a**.

To compare the regional features of precipitation over southern Asia, **Fig. 4c** shows the averaged precipitation between 10N and 20N from 40E to 180. The figure indicates that the earliest precipitation with the criterion of monsoon onset starts from early May at the southwest ICP (100E). After that the monsoon precipitation happens over the central SCS (110-120E)

(a) CMAP, 70-90E



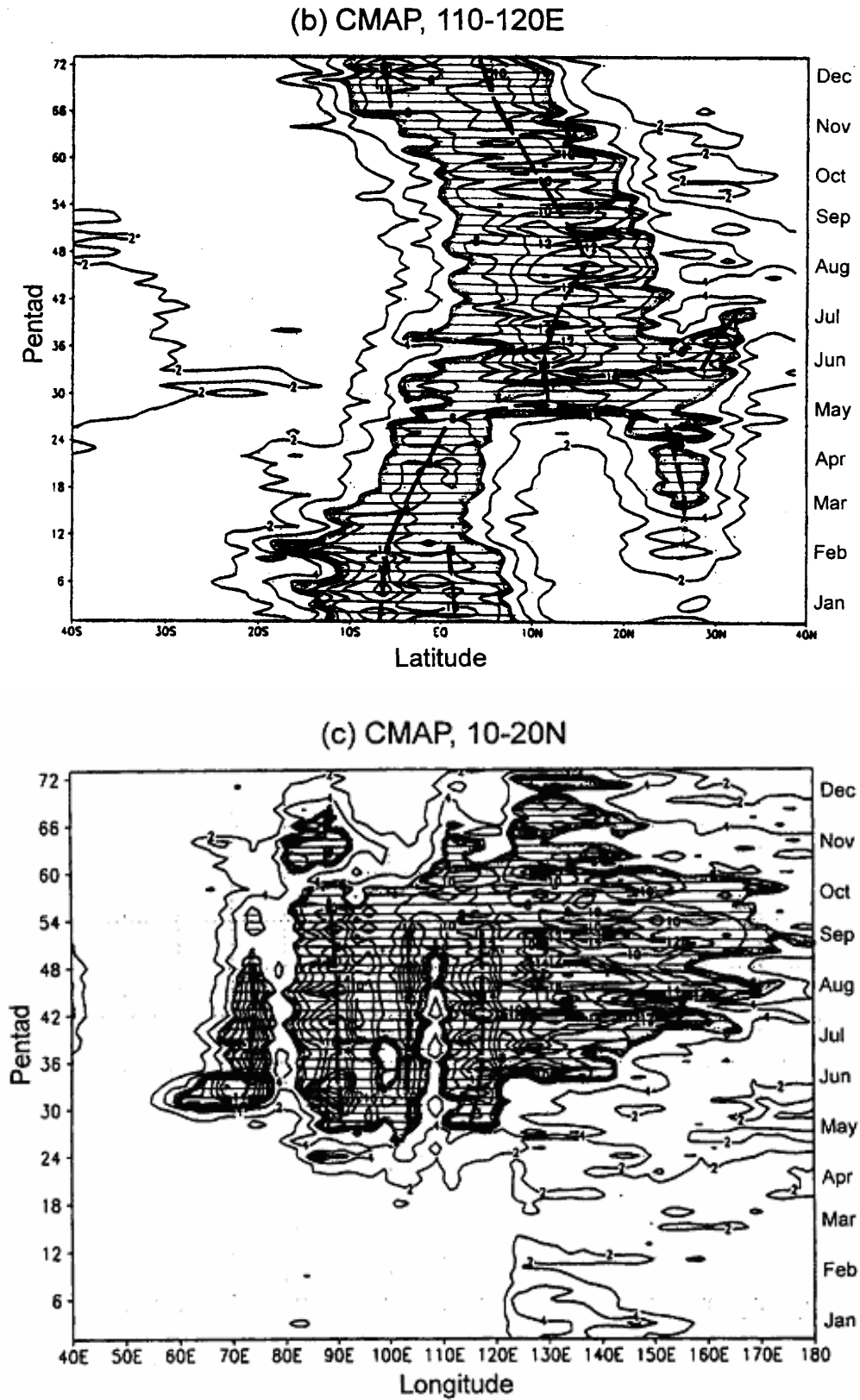


Fig. 4 The mean precipitation (mm/day) time-latitude sections from 40S to 40N averaged (a) between 70E and 90E and (b) between 110E and 120E, and (c) time-longitude section from 40E to 180 averaged between 10N and 20N. Shaded areas denote the precipitation more than 6mm/day. The dashed lines indicate the precipitation maximum.



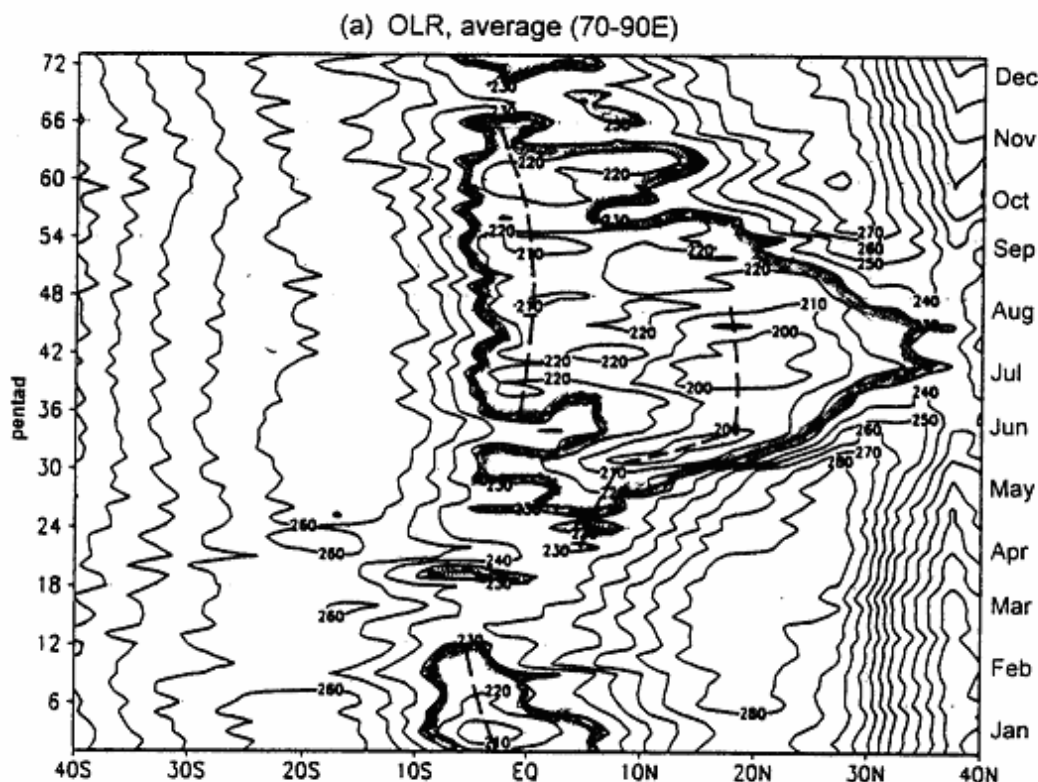
and BOB (90E) around mid-May. In early June, monsoon precipitation appears over the Arabian Sea (70E). The monsoon precipitation extends eastward to the east Philippines between 120E and 140E in mid-June, and between 140E and 160E in mid July. In southern Asia the pattern is characterized by four maxima of the rainfall that are located near the 73E, the 90E, the 105E, and the 117E, respectively. These positions roughly mark the west coasts of the Indian Peninsula, Myanmar, Cambodia and Philippines. The regional independence of monsoon precipitation is obviously manifested in these areas. This interesting fact may result from the local interaction between south-westerly monsoon flow and local topography/heating forcing or as a standing wave existing in the monsoon system.

#### 4.2 OLR

Figure 5 shows the distributions of OLR along different latitude and longitude sections with time. The averaged OLR between 70E and 90E with totally 73 pentads a year is shown in Fig. 5a. The basic consistency between Fig.5a and Fig. 4a is noted. The "Y" pattern of precipitation can also be observed in the OLR evolution, especially for the onset of the Indian summer monsoon in early June. Fig. 5b shows the averaged OLR between 110E and 120E along the

SCS longitude from 40S to 40N. Figs.5b and 4b are basically similar to an inverted "Y" pattern in the equatorial and the low-mid latitude regions but the northern band of OLR is displaced northward from the rainfall maximum. After the onset of SCS summer monsoon the Meiyu is indicated by OLR near 32N similar to but apart from the north band of the rainfall pattern.

Fig. 5c shows the averaged OLR between 10N and 20N from 40E to 180. The shaded outline of OLR is very similar to that in Fig. 4c. From Fig. 5c, the earliest monsoon onset starts around 100E near the ICP then evolves both westward and eastward. Between 70E and 90E over the India, low OLR (less than  $230\text{Wm}^{-2}$ ) starts abruptly in the pentad 31 while OLR over the central SCS (110E-120E) and the Philippines (120E-140E) and east of the Philippines (140E-160E) begins from mid May, mid June and mid July respectively. However, the internal distributions of OLR are slightly different from the precipitation. In Fig.5c, three low values lined OLR near the 75E, the 95E, and the 120E are different from the four rainfall maxima shown in Fig. 4c. Therefore, in the tropical and subtropical areas some differences are found from both distributions of OLR and CMAP.



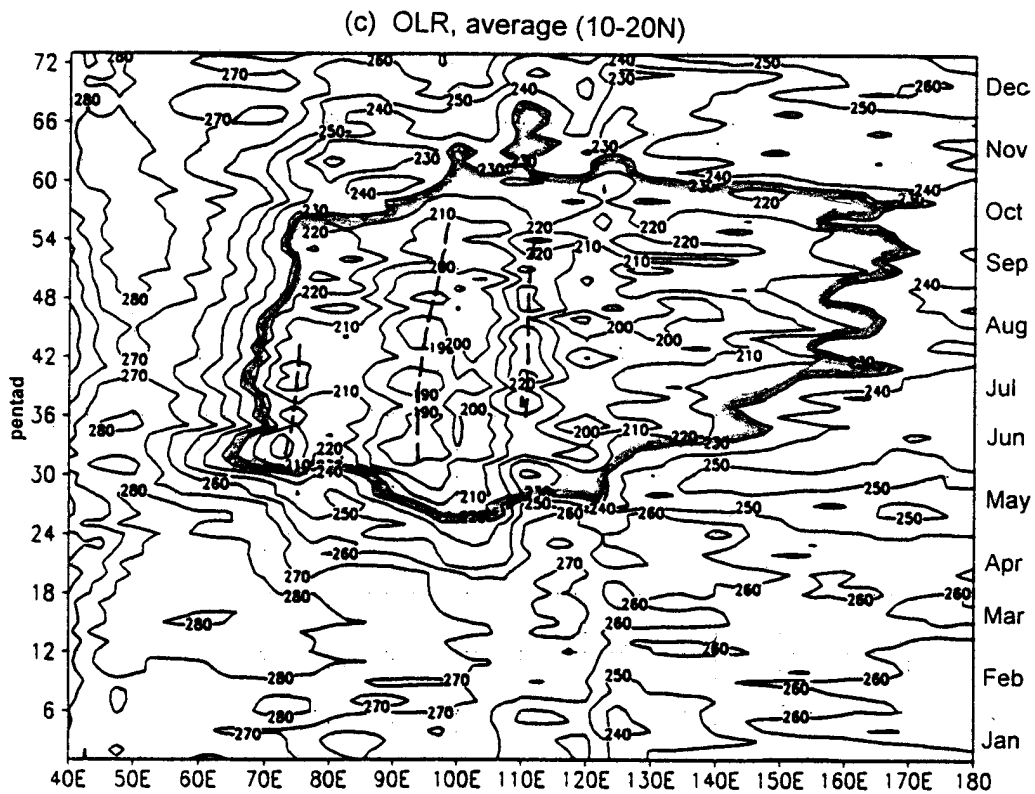
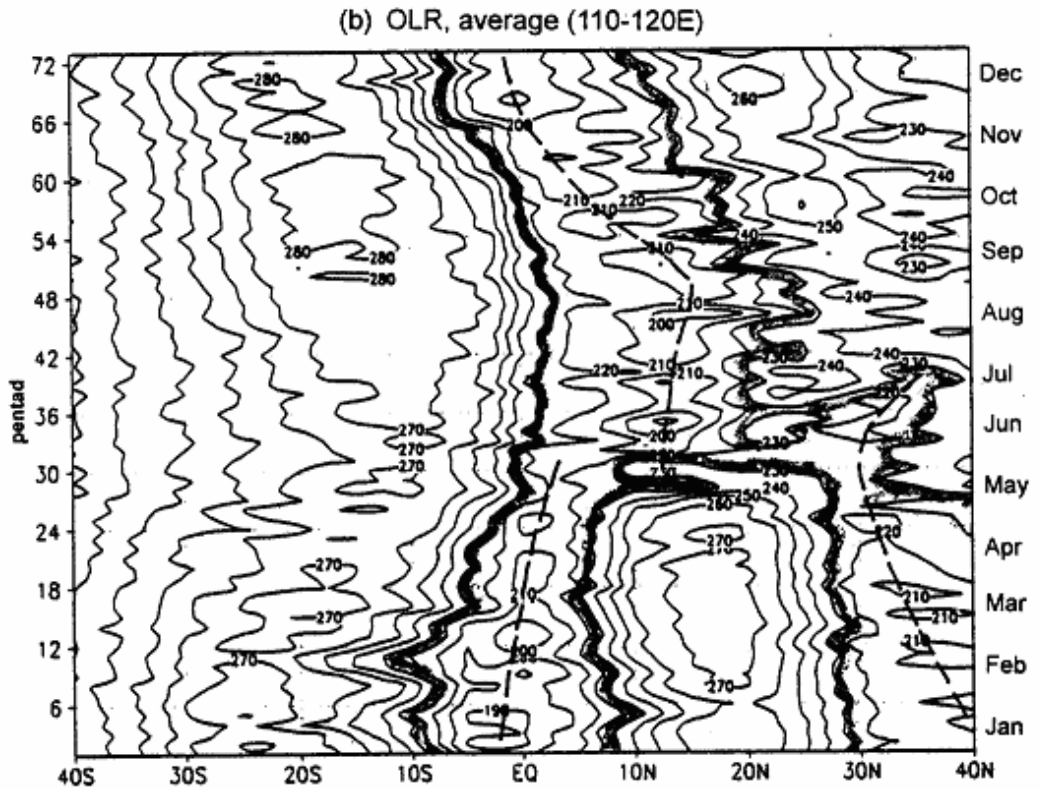


Fig. 5 Same as in Fig. 4 except the mean OLR ( $W/m^2$ )  
 Shaded areas denote the OLR less than  $230 W m^{-2}$ , the dashed lines indicate the OLR minimum.

### 4.3 BT

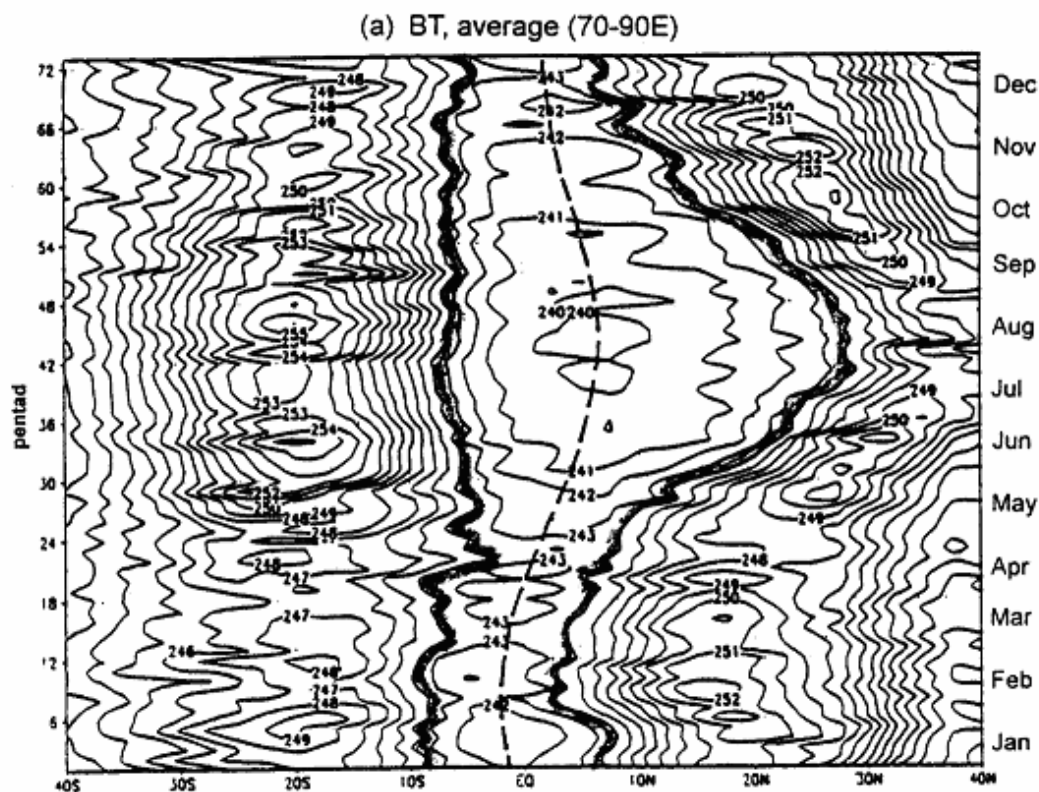
Figure 6 shows the BT distributions at different longitude and latitude sections with time. The BT distribution contains much less structure than either precipitation or OLR. Shown in Fig.6a, the shaded outline of BT distribution is similar to that of the precipitation and the OLR but no "Y" pattern can be found. In Fig. 6h two distinct features are the inverted "Y" pattern and an abrupt change in BT to values less than 244K around mid May over the central SCS. As described in section 2 the BT can indicate both a moisture upper troposphere and vertical motion but this indicator is relatively smoother than precipitation and OLR. When the strong ascending motion appears over the summer monsoon region in the Northern Hemisphere, strong descending motion occurs over the Southern Hemisphere. The moisture atmosphere over the Indian and the SCS regions gradually move northward from winter near the equator to summer at 7N. Near the equator there is no dry/wet transition through the year.

The basic outline in Fig.6c for the BT distribution is similar to those of precipitation and OLR. Onset date of the summer monsoon at different longitudes in the subtropical region between 10N and 20N can be clearly compared to each other using precipitation, OLR and BT indices. BT in Fig. 6c does not display

the standing wave like the precipitation shown in Fig.4c. Therefore, BT only shows the averaged distribution of water vapor over moisture upper troposphere.

### 4.4 Zonal Wind

The distribution of zonal wind (U-component) is shown in Figure 7. The averaged wind velocity between 70E and 90E along the Indian subcontinent from spring to summer is shown in Fig.7a. The transition position from easterly and westerly winds or shear position near 5S gradually moves northward from spring to summer. The position represents the northward shift of the cross-equatorial gyre with season. This shift is consistent with the movement of rainfall maximum from boreal spring to summer. Another feature is that the position of maximum convergence of westerly or maximum shear gradually moves northward from the equator in spring to the 20N in mid-June. This shift of position is consistent with that of the rainfall for the period so that the "Y" pattern can also be observed in Fig. 7a. Along the SCS longitude the basic features of averaged zonal wind between 110E and 120E can be noted in Fig. 7b where the maxima of velocity are indicated by dashed lines. The distribution of these dashed lines is particularly similar to that of CMAP in the period



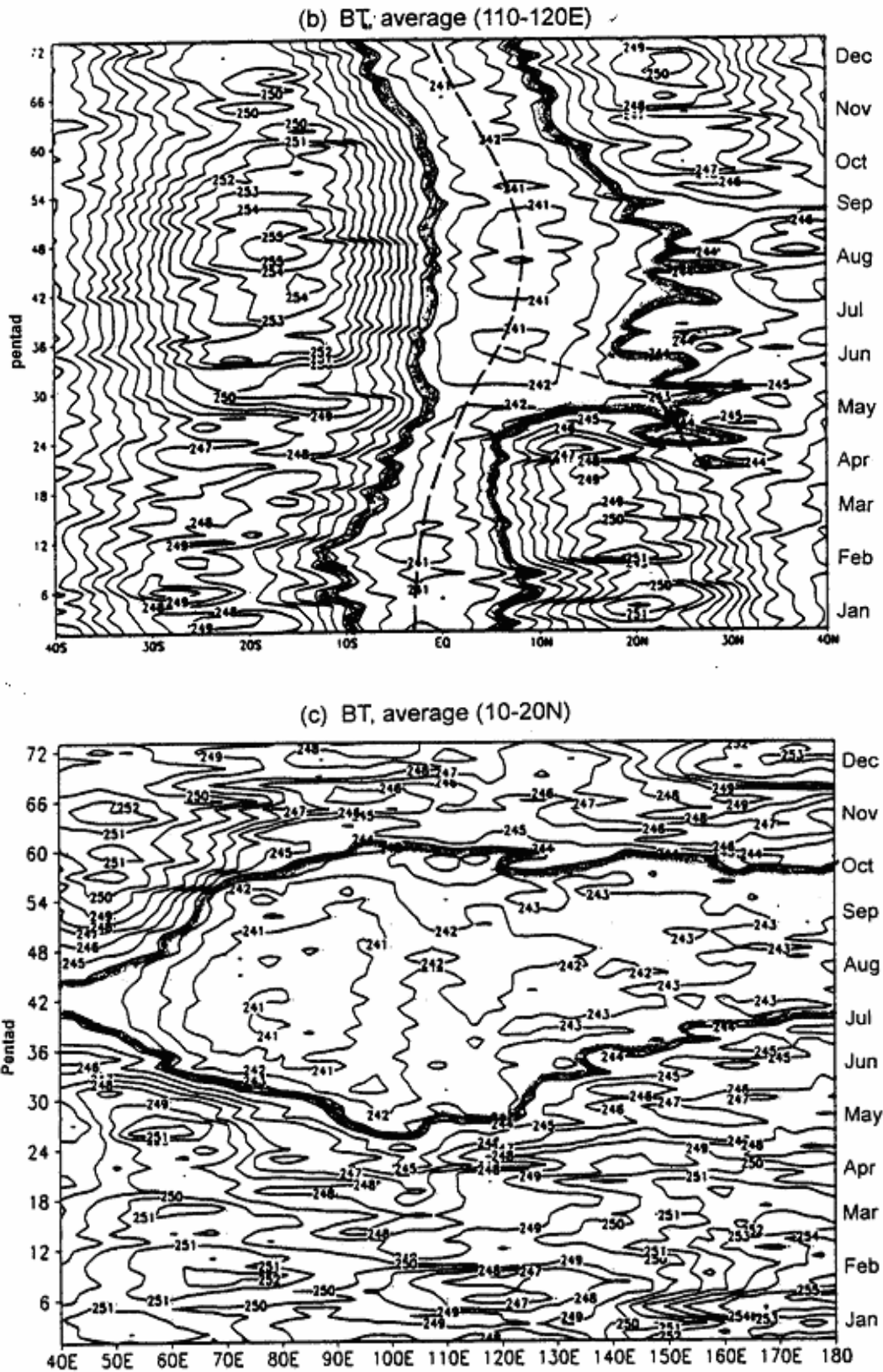
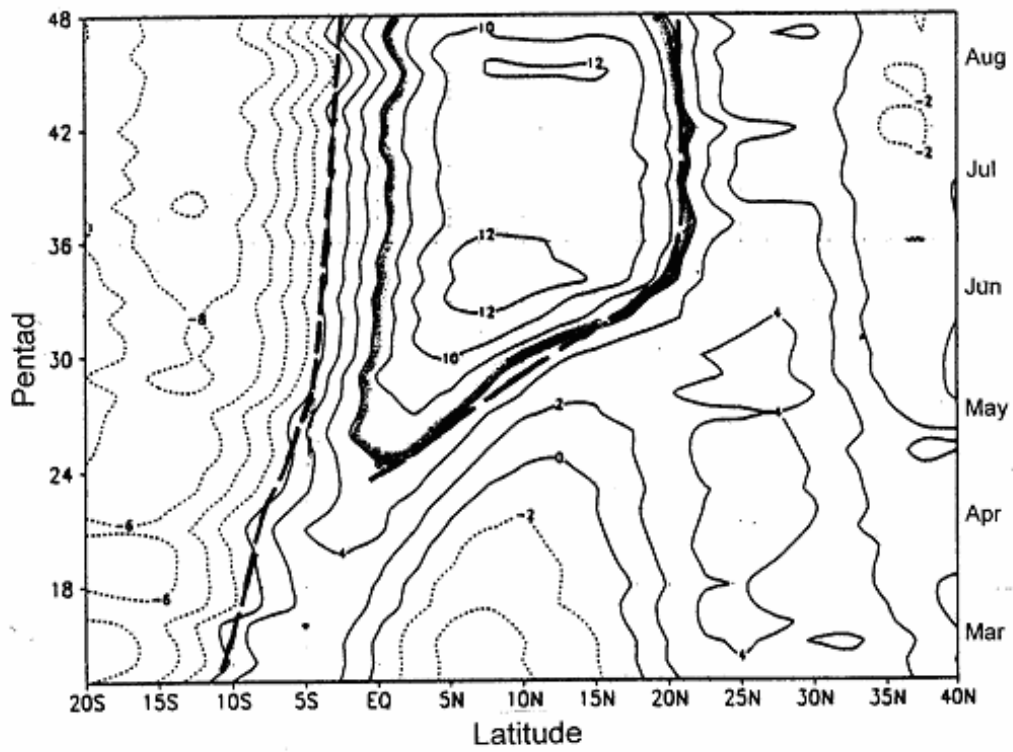
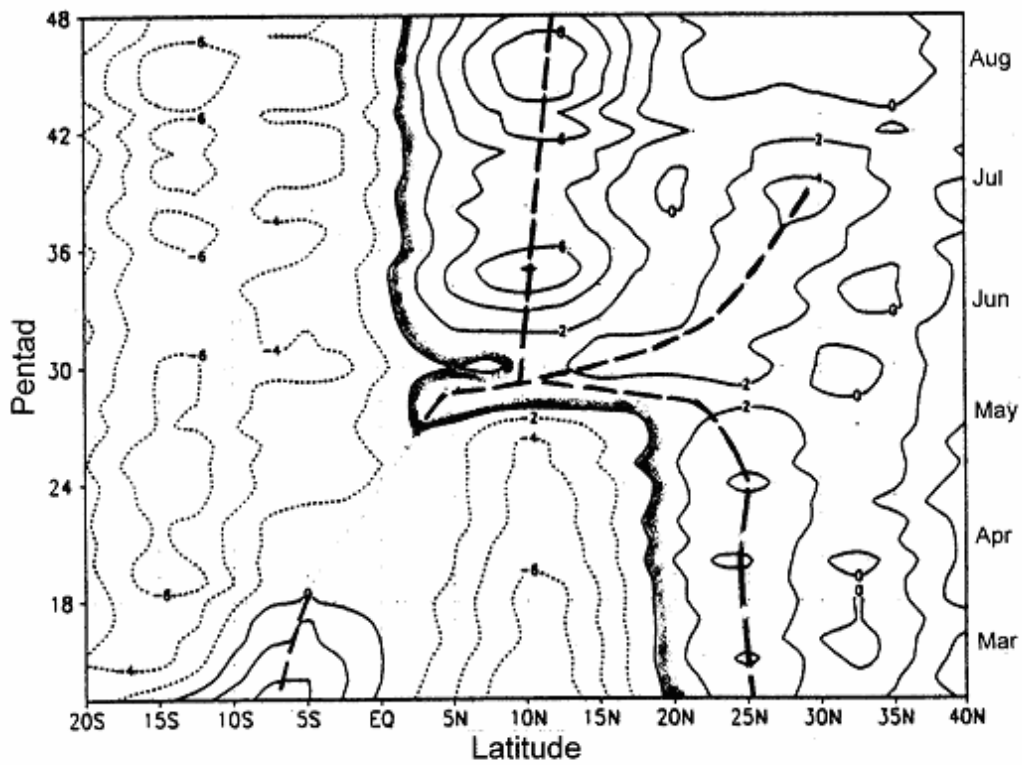


Fig. 6 Same as in Fig. 4 except the mean BT (K)  
 Shaded areas denote the BT less than 244K, The dashed lines indicate the BT minimum.

(a) 850hPa U, 70-90E



(b) 850hPa U, 110-120E



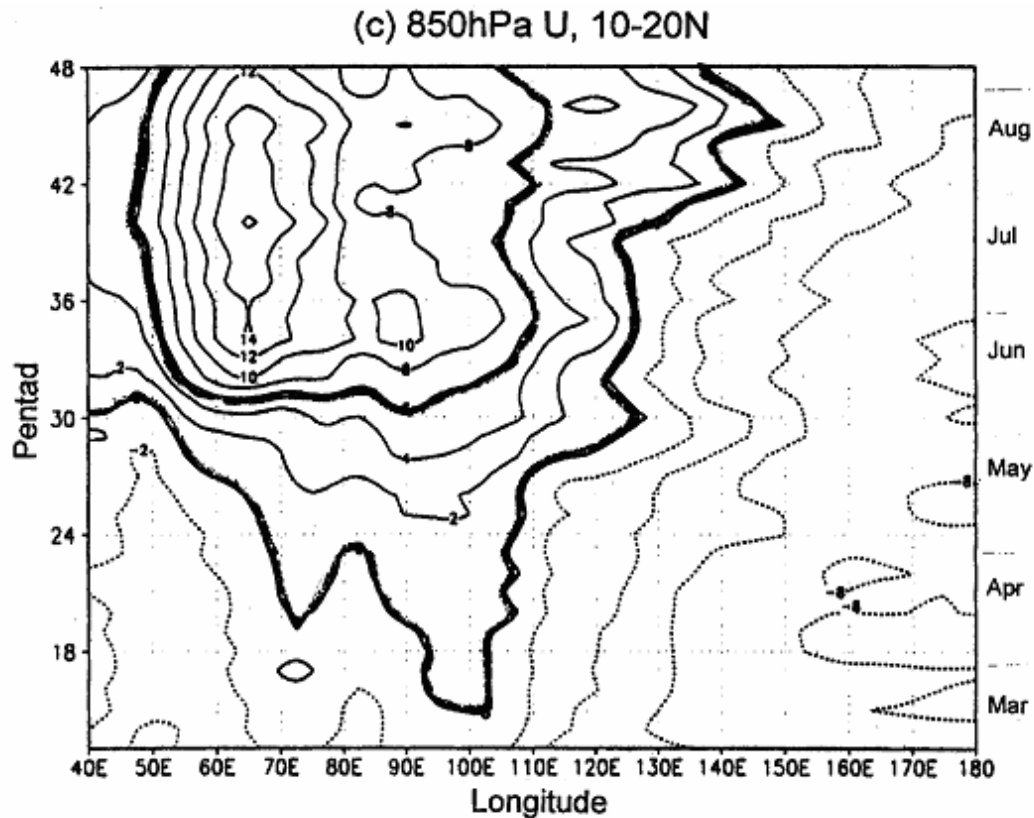


**Fig. 7** Same as in Fig. 4 except the 850hPa wind velocity (U component, m/s)  
The dashed lines indicate the wind velocity maximum or the criterion value.

from March to August shown in Fig. 4b. In the pentad 28, the wind direction abruptly changes over the central SCS and is a mark of summer monsoon onset. Before the onset of SCS summer monsoon, easterly wind prevails over the SCS region while westerly wind prevails over South China. After the SCS summer monsoon onset, the westerly wind increases along 10N over the central SCS while another westerly maximum shifts northward to central eastern China over the lower Yangtze River. For the latter, it is a mark of Meiyu onset from mid-June to mid-July. Fig.7c shows the distribution of averaged zonal wind between 10N and 20N from 40E to 180. The earliest westerly wind appears over the ICP along 100E in late March. In April, the westerly wind spreads westward to the BOB and the Arabian Sea. In mid-May, the westerly wind rapidly expands eastward to the SCS region. The Indian summer monsoon can be identified from Fig. 7c as the date when westerly wind increases to 6ms-1 in pentad 31 of the year. After the onset of the Indian summer monsoon, the strong westerly maxima are located in the west of the strong rainfall.

## 5. Conclusions

In this paper, a comparison study is carried out on the regional summer monsoon components in South

Asia and East Asia by analyzing CMAP, OLR, BT, and wind datasets. Conclusions are highlighted as follows.

(1) From winter to summer, the atmospheric circulation systems exhibit obviously seasonal transition in the Asian monsoon area, in which a series of abrupt changes occur in atmospheric systems, marking the end of the winter monsoon and the beginning of the summer monsoon. This transition abruptly appears in the pentad 28 when the SCS summer monsoon onset occurs. Before the onset of SCS summer monsoon, four rain zones are surrounded in the central SCS region. The nature of rainfall in its north is different from those in its west, south, and east. After the onset of the SCS monsoon, the monsoon rainbelt forms from the Arabian Sea through the BOB, the SCS to the northwest Pacific, associated with the southwesterly monsoon flow, oriented along this direction simultaneously. The southwesterly monsoon flow connects the South Asian and East Asian monsoons and they advance northward together.

(2) Summer monsoons act somewhat independently in South Asia, East Asia and particularly over the central SCS, South China, the ICP, the BOB, the

Indian subcontinent, and the Arabian Sea. The measurements or indices of precipitation, convection, and the winds can characterize the monsoon activities. Among the regions, the most rapid change in monsoon development occurs in the region of central South China Sea (10N-20N, 110E-120E) and another region is India. There is no dry/wet transition of monsoon over the southern SCS near the equator and the equatorial Indian Ocean. The "independence" of monsoon activities in one region from the others may be a response to the local circulation caused by the regional heating contrast or topography.

(3) The monsoon onset over the central SCS results from the combination of the tropical deep convective rainfall from the equator and the subtropical frontal rainfall over South China. Thus, an inverted "Y" pattern of precipitation and circulation can be found in East Asia. After the SCS summer monsoon onset, another band of the convective rainbelt rapidly extends northward from the central SCS to the Yangtze River and consequently the Meiyu is established over the central eastern China. The onset date of the whole Indian summer monsoon is around the 31st pentad (early June). The convective precipitation over the India is characterized by "Y" pattern emanating from the equator during the transition season. In South Asia and Southeast Asia four maxima of the rainfall are located near the 73E, the 90E, the 105E, and the 117E, respectively. These positions roughly mark the west coasts of the Indian Peninsula, Myanmar, Cambodia and Philippines during the period of summer monsoon. In the subtropical western Pacific, the monsoon precipitation extends eastward to the east Philippine between 120E and 140E in mid-June, and between 140E and 160E in mid-July.

(4) Through the comparison of the four data sets, the upper tropospheric water vapor band brightness temperature (criterion: 244K) can be used to represent the onset of summer monsoon over tropical areas and subtropical regions, but it is too smooth to represent intra-seasonal detail compared to other data sets. CMAP data (criterion: 6mm/day) can well reveal the local features of monsoon rainfalls. The OLR ( $230\text{W/m}^2$ ) can only be used to depict the convection of tropical regions but the positions between OLR and precipitation are not always consistent to each other. The distribution of wind field at the 850hPa is useful for diagnosing and explaining the development of convective precipitation but the wind alone is insufficient to describe the onset of summer monsoon. Thus, in order to judge whether the summer monsoon has happened in a local place, the moisture atmosphere or low BT expansion from the equatorial region should be analyzed except for the analysis of precipitation and wind.

## 6. Acknowledgments

The authors wish to thank Dr. P.P. Xie for providing CMAP dataset used in this paper. This study is jointly supported by the Chinese Academy of Sciences under the project number "ZKXC2-SW-210" and the National Natural Foundation of China (Contract No.49975023).

## References

- Bates, J.J., Wu, X., Khalsa, S.J.S., 1996, Interannual variability of upper-troposphere water vapor band brightness temperature. *J. Climate*, v.9, p. 427-438
- Ding, Y.H., Wang, Q., and Yan, J., 1996, Some aspects of climatology of the summer monsoon over the South China Sea. In: *From Atmospheric Circulation to Global Change*, Ed. by IAP Chinese Academy of Sciences, China Meteorological Press, p.329-339
- Jin, Z.H., 1999, The climatic characteristics of summer monsoon onset over the South China Sea based on TBB data. In: *Onset and evolution of the South China Sea monsoon and its interaction with the ocean*, Ed. By Ding Y. and Li C., China Meteorological Press, p.264-271
- Kang I.-S., Ho C.-H., Lim Y.-K., and Lau K.-M., 1999, Principal modes of climatological seasonal intraseasonal variations of the Asian summer monsoon. *Mon. Wea. Rev.*, v. 127, p.322-340
- Krishnamurti, T.N., 1985, The Summer Monsoon Experiment, A review. *Mon. Wea. Rev.*, v.113, p.1509-1626
- Lau K.-M., Kim K.-M., and Yang S., 2000, Dynamical and boundary forcing characteristics of regional components of the Asian summer monsoon. *J. Climate*, v.13, 2461-2482
- Lau, K.-M. and Li, M.T., 1984, The monsoon of East Asia and its global association. *Bull. Amer. Meteor. Soc.*, v.65, p.114-125
- Lau, K.-M., Yang, G. J. and Shen, S. H., 1988, Seasonal and interseasonal climatology of summer monsoon rainfall over East Asia. *Mon. Wea. Rev.*, v.116, p.18-37
- Lau, K.-M., and Yang, S., 1997, Climatology and interannual variability of the Southeast Asian summer monsoon. *Adv. Atmos. Sci.*, v.14, p.141-162
- Qian, W.-H., and Lee, D. K., 2000, Seasonal march of Asian summer monsoon. *Int. J. Climatol.*, v.20, p.1371-1386
- Qian, W.-H. and Yang, S., 2000, Onset of the regional monsoon over Southeast Asia. *Meteorol. Atmos. Phys.* v.74(5), p.335-344
- Qian, W.-H., Deng, Y., Zhu, Y., and Dong, W., 2002, Demarcating the worldwide monsoon. *Theor. Appl. Climatol.* V.71, p.1-16
- Qian, W.-H., Zhu, Y.-F., Xie, A., and Ye, Q., 1998, Seasonal and interannual variation of upper tropospheric water vapor band brightness temperature over the global monsoon regions. *Adv. Atm. Sci.*, v.15, p.337-345
- Tao, S.-Y., and Chen. L.-X., 1987, A review of recent research on the East Asian summer monsoon in China. In: *Monsoon Meteorology*, Ed. By C.-P. Chang and T. N. Krishnamurti, Oxford University Press, pp.60-92.
- Wang, S.-Y., and Qian, Y.-F., 1999, Basic features of regional heating field before and after the onset of the South China Sea

- monsoon in 1998. Onset and evolution of the South China Sea monsoon and its interaction with the ocean, Ed. By Ding Y. and Li C., China Meteorological Press, pp.235-246.
- Webster, P. J., 1987, The elementary monsoon. *Monsoons*, John Wiley & Sons, Inc. pp.3-32.
- Webster, P. J., and Yang, S., 1992, Monsoon and ENSO: Selectively interactive systems. *Q. J. R. Meteorol. Soc.*, v.118, p. 877-926
- Wu, G.X., and Zhang, Y. S., 1998, Tibetan Plateau forcing and the timing of the monsoon onset over South Asia and the South China Sea. *Mon. Wea. Rev.*, v. 126, p. 913-927
- Wu, X., Bates, J. J., and Khalsa, S. S., 1993, A climatology of the water vapor band brightness temperatures from NOAA operational satellites. *J Climate*, v.6, p.1282-1300
- Xie, A., Chung, Y.-S., Liu, X. and Ye, Q., 1998, The interannual variability of the summer monsoon onset over the South China Sea. *Theor. Appl. Climatol.*, v.59, p.201-213
- Xie, P. and Arkin, P. A., 1997, Global precipitation: A 17-year monthly analysis based on gauge observations, satellite estimates, and numerical model output. *Bul. Amer. Meteor. Soc.*, v. 78, p.2539-2558
- Yang S., and Gutowski W.J., 1992, On the relationship between tropical Chinese rainfall and the Indian summer monsoon. *J. Meteor. Soc. Japan*, v.70, p.997-1004